

Pharmacodynamic Evaluation of AUM001/Tinodasertib, an Oral Inhibitor of Mitogen-Activated Protein Kinase (MAPK)-Interacting Protein Kinase 1,2 (MNK1/2) in Preclinical Models and Tissues from a Phase 1 Clinical Study

Bong Hwa Gan¹, Lay Hoon Lee¹, Reika Takeda¹, Maryam Yasin¹, Vincenzo Teneggi¹, Kantharaj Ethirajulu¹, Pauline Yeo¹, Dhananjay Umrani¹, Vishal Pendharkar¹, Darren Wan Teck Lim², Greg Li², Qingshu Lu³, Yang Cao³, Ranjani Nellore¹, Stephanie Blanchard¹, Hannes Hentze¹, Veronica Novotny-Diermayr^{1*}

Abstract

Mitogen-activated protein kinase (MAPK) interacting kinase (MNK) inhibitors affect cap-dependent mRNA translation by blocking the phosphorylation of RNA-binding proteins such as the eIF4E. Phosphorylation on S209 of eIF4E (p-eIF4E) causes hyperactivation and dysregulation of mRNA translation, which is a hallmark of numerous malignancies. AUM001/Tinodasertib (ETC-206) is a selective and potent oral kinase inhibitor of MNK1 and MNK2 (IC₅₀ of 64 and 86 nM, respectively), inducing dose-dependent inhibition of p-eIF4E with an IC₅₀ of 0.8 μM in K562-eIF4E cells. In mice, single oral doses of ~12.5 mg/kg led to rapid (1-2 h post-dose) ~70% inhibition of p-eIF4E in different normal or tumor tissues at a plasma concentration of 8.6 μM. However, in PBMCs obtained from human healthy volunteers in a Ph1 study, single oral doses of 10 or 20 mg ETC-206 did not show inhibitory activity up to 12 h post-dose, instead ETC-206 caused a statistically significant (p=0.0037) p-eIF4E inhibition in PBMCs of 24% at 24 h post-dose with 10 mg, and an inhibition of ≥27% up to 52% was seen in 11/14 subjects in the 20 mg group where ETC-206 plasma concentrations remained above the IC₅₀ for p-eIF4E (1.7 μM) for 30 h. While in mouse pharmacodynamic (PD) activity was also shown in tumor, skin, and hair follicles, in human tissues, PBMCs showed a trend for delayed PD inhibition and skin was not a suitable surrogate. Analysis of pharmacokinetic (PK) and PD relationships shown herein demonstrate excellent pharmaceutical properties of ETC-206 which has now advanced to Ph2 clinical trials (NCT05462236).

Keywords: MNK; eIF4E; mRNA translation; Oral kinase inhibitor; Pharmacodynamics; Pharmacokinetic; Mouse; Human; Clinical.

Introduction

MNK1 and MNK2 are serine-threonine kinases of the MAPKs family [1] which are activated via phosphorylation on threonine (Thr) 197/202 by the MAPKs ERK and p38. MNKs are the sole kinases known to phosphorylate the eukaryotic initiation factor 4E (eIF4E) on Ser209 [2], and are a part of the large eIF4F complex, playing a central function in cap-dependent mRNA translation. MNKs need to be in physical proximity to eIF4E for the Ser209 phosphorylation to take place, which is achieved by binding to the scaffolding protein eIF4G, another component of the eIF4F complex.

Affiliation:

¹Experimental Drug Development Centre (EDDC), Agency for Science, Technology and Research (A*STAR), Singapore

²SingHealth Investigational Medicine Unit, Singapore

³Singapore Clinical Research Institute (SCRI), Singapore

*Corresponding author:

Veronica Novotny-Diermayr, Experimental Drug Development Centre (EDDC), Agency for Science, Technology and Research (A*STAR), Singapore

Citation: Bong Hwa Gan, Lay Hoon Lee, Reika Takeda, Maryam Yasin, Vincenzo Teneggi, Kantharaj Ethirajulu, Pauline Yeo, Dhananjay Umrani, Vishal Pendharkar, Darren Wan Teck Lim, Greg Li, Qingshu Lu, Yang Cao, Ranjani Nellore, Stephanie Blanchard, Hannes Hentze, Veronica Novotny-Diermayr. Pharmacodynamic Evaluation of AUM001/Tinodasertib, an Oral Inhibitor of Mitogen-Activated Protein Kinase (MAPK)-Interacting Protein Kinase 1, 2 (MNK1/2) in Preclinical Models and Tissues from a Phase 1 Clinical Study. *Journal of Cancer Science and Clinical Therapeutics*. 8 (2024): 254-264.

Received: July 23, 2024

Accepted: July 29, 2024

Published: August 16, 2024

The affinity of MNKs to eIF4G in turn is regulated by a Pak2-mediated phosphorylation of MNK1 on Thr22/Ser27 [3], thereby adding an additional level of regulation to the phosphorylation of eIF4E [4, 5]. MNK inhibitors were initially of interest because eIF4E was described as a bona-fide oncogene with phospho-(p)-Ser(S)209-eIF4E being necessary for tumorigenesis but dispensable for normal development [6-9]. Knock-in studies with a S209A mutant of eIF4E further confirmed that a loss of Ser209 phosphorylation does not cause developmental defects or a loss of cell viability [10], while a multitude of independent studies demonstrated that increased levels of p-S209-eIF4E were linked to poor prognosis in a variety of different cancers [11, 12], promoted epithelial to mesenchymal transition, invasion and metastasis [13]. However, the interest in targeting MNKs has picked up because it was noted that a decrease of p-S209-eIF4E due to MNK inhibition specifically and disproportionally affecting the translation of a subset of mRNAs that promote cell survival, cytokines, tumor growth and invasion, while not affecting global protein translation. Among the differentially translated proteins in tumors is the programmed death ligand 1 (PD-L1) [9, 10, 14, 15]. Recently, studies demonstrated that cap-dependent mRNA translation plays an important role in a multitude of cells of the tumor microenvironment with levels of p-S209-eIF4E causing differential effects in neutrophils, macrophages, regulatory T-cells and Th1 cells and T-cells, affecting cell survival and cytokine production [16-18], giving rise to the hypothesis that MNK inhibitors in combination with immunotherapy will potentially provide effective treatment options for cancer. Tomivosertib (eFT508; Effector Therapeutics Inc.) was the first highly selective small molecule inhibitor of MNK1/2 with *in vitro* potency in the nanomolar range that entered into clinical studies [19]. In preclinical mouse models, it was demonstrated that liver tumors with a particular molecular phenotype showed a 50% reduction in p-eIF4E and PD-L1 levels after treatment with 10 mg/kg eFT508 [15]. In a Ph2a study it was demonstrated that the combination of eFT508 with PD-1/PD-L1 inhibitors led to a significant increase in progression-free survival in non-small cell lung cancer (NSCLC) patients. Recently a randomized, double-blinded, placebo controlled pivotal study has been started in the same indication [20]. ETC-206 is a small molecule MNK1/2 inhibitor of that is highly selective for MNK kinases, with an *in vitro* IC₅₀ of 64 and 86 nM for MNK1 and MNK2, respectively. ETC-206 exhibits favorable PK parameters and induced tumor regression in combination with BCR-Abl inhibitor (dasatinib) in a murine model of blast crisis chronic myeloid leukemia (CML) [1]. ETC-206 was initially assessed in a single ascending dose trial, followed by a multiple ascending dose trial, performed in human healthy volunteers (HVs). ETC-206 was shown to be safe and well tolerated [21], without any treatment-emergent adverse events or dose limiting toxicities and is

now being explored in an ongoing Ph2 trial in metastatic colorectal cancer in combination with either pembrolizumab or irinotecan (NCT05462236). Here, we describe the use of a Western blot assay to demonstrate target engagement, assess PK/PD relationships in preclinical models and compare to results obtained in a first-in-human (FIH) HV study after ETC-206 single dose.

Methods

Compounds

ETC-206 (Syngene International Ltd, Bengaluru, India) was prepared for *in vitro* studies as a 10 mM stock in DMSO. For oral administration in animals, ETC-206 was prepared in sodium carboxymethyl cellulose (Na-CMC) containing 0.5% Tween® 80, to yield a 99.5% (w/v) Na-CMC suspension that was vortexed, sonicated, and dosed at 10 mL/kg. ETC-206 for human oral ingestion was formulated as 10 mg strength in white, opaque capsules with matching placebo capsules and manufactured at Patheon UK Ltd (Milton Park, United Kingdom).

Phase 1 healthy volunteer study

Biomarker samples i.e. hair follicles (HFs), peripheral blood mononuclear cells (PBMCs), skin biopsies were collected from a total of 23/24 subjects recruited in a Ph1 study conducted in Singapore (IRB approval #2016/2522) described earlier [21]. Participants provided informed consent before starting any study-related procedure, and the patient recruitment period for this study was from 22 Sept 2016 until 4 April 2017 (last patient visit). See *Supplementary Methods* for details of sample collection/processing.

Cell lines, primary cells, and cell lysis

The human chronic myeloid leukemia (CML) cell line K562 (#CCL-243™, American Tissue Type Collection [ATCC]) was batch-transfected with the MSCV-IRES-GFP vector ENREF76 [9], encoding full-length murine eIF4E (named K562-eIF4E). Transfected cells were FACS-sorted for cells expressing high levels of eIF4E. Cells were grown according to ATCC's instructions and authenticated by Axil Scientific (Singapore). PBMCs were obtained from healthy donors under IRB approval #NUS2110 or during the ETC-206 clinical study (IRB approval #2016/2522), collected using Vacutainer CPT™-tubes (#362761, Becton, Dickinson and Company), washed and plated in 6-cm cell culture dishes in RPMI 1640 containing 10% FBS and 1% penicillin-streptomycin solution, and maintained at 37°C and 5% CO₂ for 2-3 h or overnight prior to treatment. Cells were lysed in Complete Lysis Buffer on ice, prepared by adding HALT™ protease and phosphatase inhibitor cocktail (#78440) to a final of 1X concentration to Pierce® RIPA buffer (#89900), from Thermo Fisher Scientific.

Animal studies

All rodents (InVivos, Singapore) were housed in individual ventilated cages under controlled conditions, in compliance with NIH and NACLAR guidelines. Experiments were performed under IACUC Approval #151001. Mice between 6 and 12 weeks of age were used. PK/PD studies were performed in non-tumor-bearing female ICR mice (IcrTac:ICR or Hsd:ICR(CD-1[®]), or in female SCID mice (C.B-IgH-1^b/IcrTac-Prkdc^{scid}) bearing K562-eIF4E xenografts as described previously [1]. After ~12 days, when tumors reached a volume of ~200-500 mm³, animals received a single dose of ETC-206, and tissues were harvested at different time points post-dose. Tumor volumes were calculated in mm³ using $w^2 \times l/2$ (w = width, l = length in mm).

Tissue homogenization

Briefly, tissues (tumor, HFs, skin) were homogenized in cold Complete Lysis Buffer containing either zirconia or stainless steel beads (Tomy Digital Biology Co Ltd.) using Micro Smash[™] tissue homogenizer (Tomy Digital Biology Co Ltd.) at a speed of 4,000 rpm under external cooling using dry ice in 5 cycles of 10 s each (tumor, skin) or 3 cycles of 5 min each (HFs) followed by 1 min of cooling between cycles. After 5 min incubation on ice, lysates were cleared by a 15 min spin. Human tissues were collected from HVs in the Ph1 study previously described [21]. For detailed methods used to prepare lysates from mouse and human samples see *Supplementary Methods*.

Western blot

Total protein concentrations were determined against a standard curve of BSA in a 96-well plate using the DC[™] Protein assay (Bio-Rad Laboratories). Proteins were separated on reducing 10% NuPAGE[™] Novex[™] Bis-Tris Protein Gels and transferred onto PVDF membranes, blocked (5% BSA in 1X TBST containing 0.05% Tween-20) at room temperature, and probed overnight at 4°C with either of the following antibodies: p-S209-eIF4E (#9741), total eIF4E (#2118), all diluted 1:1,000; or GAPDH clone 14C10 (#2118) diluted 1:10,000. Secondary antibodies used were anti-rabbit-IgG-HRP or anti-rabbit-IgG-AP, (#7074, #7054) diluted 1:2,000. All antibodies were purchased from Cell Signaling Technology. For developing, either Amersham ECL[™] Prime Western Blotting Detection Reagent (Cytiva) or Immune-Star[™] AP Substrate (Bio-Rad Laboratories) were used. Images were digitally captured using Amersham Imager 600 UV (Cytiva) and analyzed densitometrically using the ImageQuant[™] TL software v8.1 (Cytiva). Relative p-eIF4E levels were determined as a ratio of p-eIF4E levels over total eIF4E measured in the same sample. To determine the percentage inhibition relative p-eIF4E levels in a sample were compared to relative levels of p-eIF4E from the same subject pre-dose (or vehicle-treated mice), set to 100%.

Bioanalysis and PK

Plasma samples were collected using K₂EDTA as anti-coagulant. Dosing solutions of preclinical experiments were diluted 8,000-fold in a 1:1 mixture of methanol and water. Mouse tissue samples (plasma, skin, tumor) were diluted 10-fold. Detailed methods for extraction and bioanalysis are provided in the *Supplementary Methods*. Bioanalysis of human plasma samples was performed blinded at SGS (Cephac, France), using an analytical validated method under GLP. PK parameters of human samples were analyzed by Phinc Development (Évry, France) using Phoenix WinNonlin[®] Professional software v6.4, Pharsight Corporation).

Statistical analyses

Statistical analyses (if not otherwise mentioned) have been performed using GraphPad Prism 7 for Windows, v7.02 (GraphPad Software Inc.). For clinical sample analysis normality was tested using the D'Agostino and Pearson omnibus normality test. Sphericity was not assumed. For PBMCs repeated measures one-way ANOVA was performed using all time points that did not have missing data, to determine significance of inhibition and to test for linear trend of inhibition. Where the data was not normally distributed, significance was determined using the Wilcoxon Matched Pairs Signed Rank Test or the values were transformed (\log_2) prior to performing the analysis.

Results

Determination of the IC₅₀ for inhibition of p-eIF4E by ETC-206 in human cells *in vitro*

ETC-206 is a potent and selective MNK1/2 inhibitor, which was confirmed in a SelectScreen[®] panel with 414 recombinant human kinases, where only 38 kinases were identified that were inhibited >50% at 10 μ M. IC₅₀ determination using the same assays for each of these 38 kinases confirmed that ETC-206 is most active against MNK1 (IC₅₀: 64 nM) and MNK2 (IC₅₀: 86 nM), with the next lowest IC₅₀ of 610 nM (S1 Table) for receptor interacting serine/threonine kinase 2 (RIPK2). ETC-206 was mildly anti-proliferative when tested using CellTiterGlo[®] luminescent cell-viability assay in a panel of 71 tumor and non-cancerous human cell lines, with cellular IC₅₀ mostly in the 10-45 μ M range, and only 5 cell lines showed inhibition <10 μ M (S2 Table). To establish the p-eIF4E inhibition as a PD target engagement biomarker, K562-eIF4E cell line and HVs' PBMCs were treated *in vitro* for 2 h with 12 nM to 50 μ M ETC-206, and p-eIF4E, eIF4E and GAPDH levels were determined by Western blot. Treatment with ETC-206 led to a concentration-dependent inhibition of relative p-eIF4E levels, where 50 μ M ETC-206 led to a \geq 90% inhibition (Figure 1). The IC₅₀ of p-eIF4E was determined to be 0.8 μ M for K562-eIF4E cells and about 2-fold higher (1.7 μ M) in primary human PBMCs. Concentrations below ~0.8 μ M (K562-eIF4E cells) or ~0.5 μ M (PBMCs) only

gave a marginal p-eIF4E inhibition. Normalizing p-eIF4E levels using total eIF4E levels gave comparable results to normalization using GAPDH levels, the latter was therefore not determined for all following studies.

Effects of ETC-206 on inhibition of p-eIF4E in mouse normal tissues

The inhibitory effect of ETC-206 on relative p-eIF4E levels in different normal (non-cancer) tissues was determined in ICR mice (Figure 2). Comparing tissue samples from mice treated for 1 h with a single dose of 200 mg/kg ETC-206 to vehicle-treated mice, an inhibition of p-eIF4E of 53% in bone marrow, 62% in PBMCs, 82% for skin, and 78% in HFs was determined (Figure 2A). In platelets, no p-eIF4E inhibition could be determined as expression of eIF4E was very low compared to other tissues (Figure 2A, bottom panel). PBMCs, skin, and HFs were chosen for further analysis of p-eIF4E

inhibition. The time point of maximum inhibition and the duration of p-eIF4E inhibition in ICR mice were determined after receiving a single dose of 200 mg/kg ETC-206. Relative p-eIF4E levels were measured at different time points post-dose in PBMCs, skin, and HFs (0.5-24 h), and compared to relative p-eIF4E levels of vehicle-treated mice, considered to be 100% at 0 h (Figure 2B). The onset of the inhibitory effect was rapid with 55-65% inhibition observed in all tissues at 0.5 h post-dose and maximum inhibition achieved at 1-2 h post-dose (~85% in skin and HFs, ~70% in PBMCs). High levels of inhibition were sustained for up to 12 h, and 24 h after a single-dose treatment with ETC-206, p-eIF4E inhibition was still between 50-65% in all three tissues when the plasma concentration was around ~5,000 ng/mL or 12 μ M (data not shown) in an independent experiment. Overall, a higher variability of p-eIF4E inhibition was observed in PBMCs compared to other tissues tested.

Effective dose range to inhibit p-eIF4E in different tissues versus plasma exposure after a single dose of ETC-206 in mice

To determine the minimal inhibitory dose of ETC-206 and the corresponding plasma concentrations *in vivo*, ICR and SCID mice received single oral doses of ETC-206, and the relative p-eIF4E levels in PBMCs, skin, HFs, and tumor samples (for SCID mice carrying K562-eIF4E tumors) were compared to vehicle-treated mice 2 h post-dose, with ETC-206 plasma concentrations analyzed in the same animals. ICR mice received 8 doses of ETC-206 (1-200 mg/kg) and SCID mice received 5 doses (12.5-200 mg/kg). ETC-206 plasma levels showed an overall similar linear dose-exposure relationship in ICR and SCID mice across the dose range tested with slightly higher ETC-206 exposure in ICR mice (Figure 3A). In ICR mice, a rapid dose-dependent decrease in relative p-eIF4E levels was observed, with a minimum inhibitory dose of approximately 12.5 mg/kg in skin, HFs and spleen (Figure 3B upper panels and S1C Figure). In PBMCs, variation was high and only the highest dose of 200 mg/kg resulted in significant p-eIF4E inhibition of ~70% (Figure 3B). In skin and PBMCs, lower doses of ETC-206 led to an increase in p-eIF4E levels beyond basal levels (~1.7-fold at the doses of 1-3 mg/kg for skin, ~2.5-fold at 6-25 mg/kg in PBMCs), yet, there was a statistically significant, strongly negative correlation between ETC-206 plasma concentrations and p-eIF4E levels in all tissues except PBMCs (Pearson's *r* between -0.75 and -0.77 compared to -0.38 in PBMCs; Figure 3B, lower panels).

Next, we assessed if p-eIF4E levels in tumor could be inhibited at a lower dose compared to non-tumor tissue. Subcutaneous K562-eIF4E tumors were grown in SCID mice as previously described [1]. In this mouse model of human blast crisis CML ETC-206 was previously shown to have

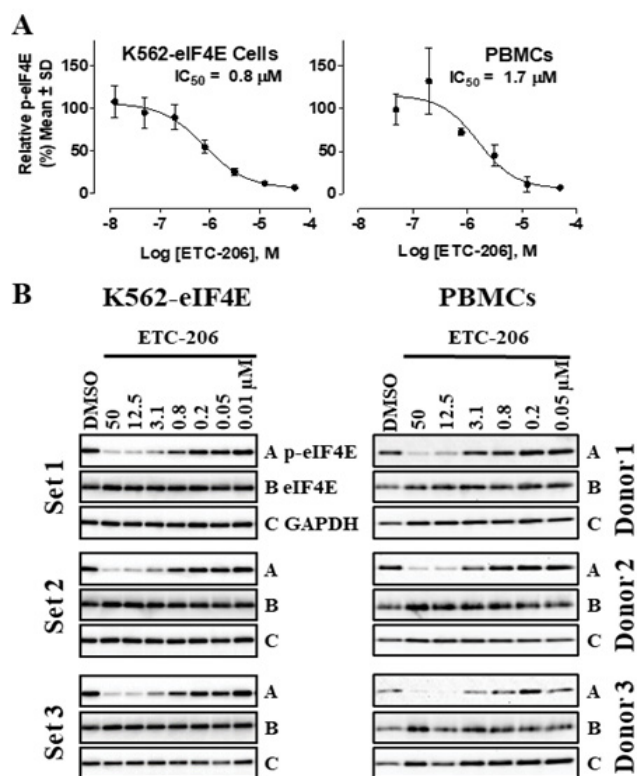


Figure 1: ETC-206 inhibits p-eIF4E in human cells *in vitro*. K562-eIF4E cells or primary human PBMCs obtained from volunteer donors were treated with different concentrations of ETC-206 or vehicle control (0.1% DMSO) as indicated for 2 h. Cells were lysed, separated on Bis-Tris protein gels, and Western blot analysis was performed using antibodies against p-eIF4E, eIF4E, and GAPDH as indicated. (A) IC₅₀ curves showing relative p-eIF4E levels in K562-eIF4E cells and in PBMCs. Relative p-eIF4E levels were determined densitometrically from Western blots to calculate IC₅₀ values; For K562-eIF4E cells n=6; "Set 1" refers to one sample set from those 6 replicates. (B) Corresponding Western blots from one half of the experiments (n=3) is shown; 5 μ g/10 μ g of protein loaded per lane for K562-eIF4E cell line/PBMCs, respectively.

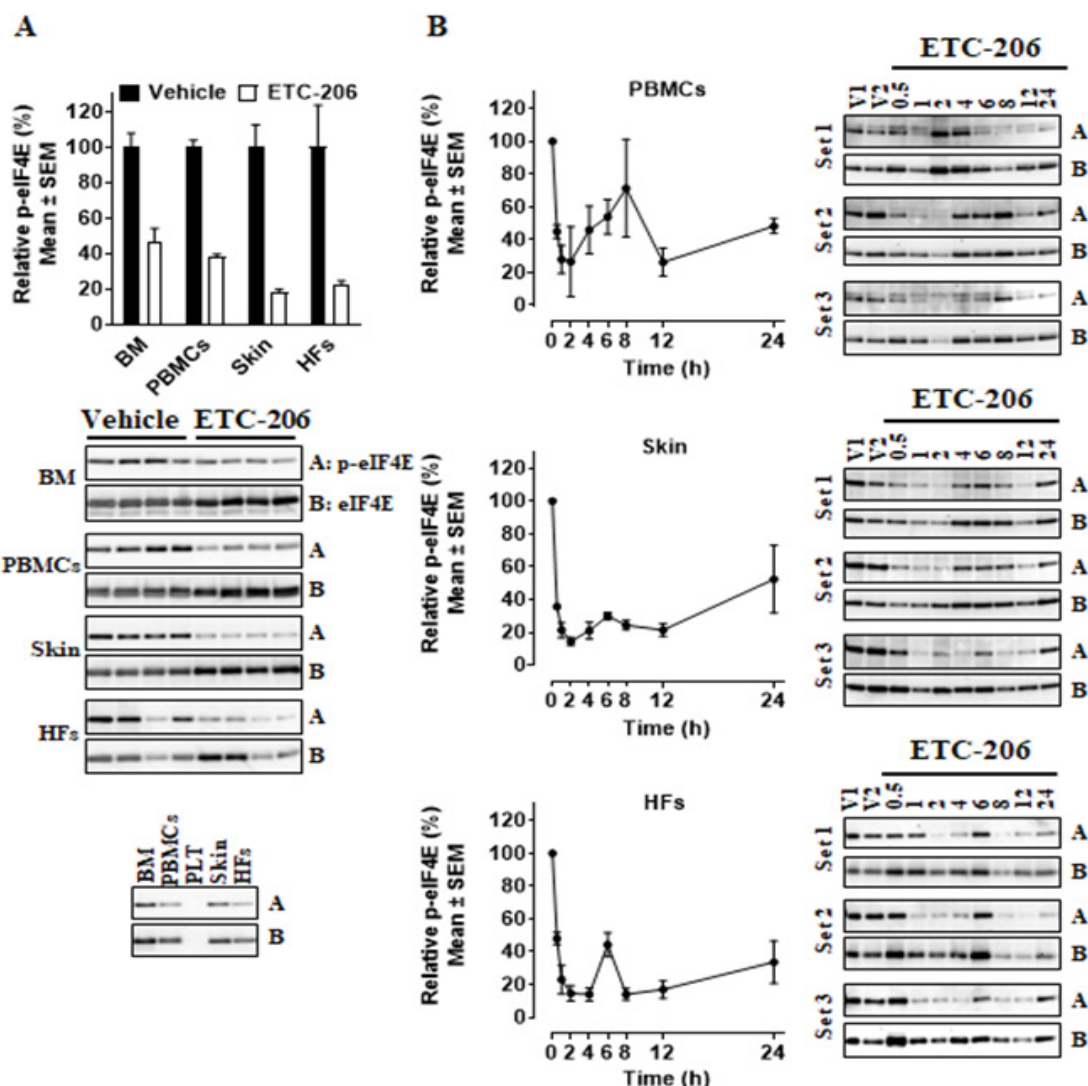


Figure 2: Inhibition of eIF4E phosphorylation by single-doses of ETC-206 in surrogate tissues from ICR mice. Female ICR mice were dosed orally with a single dose of vehicle or 200 mg/kg ETC-206 (n=4/group). (A) Mice were euthanized, and tissues collected 1 h post-dose. Tissue samples from surrogate tissues were analyzed via Western blot analysis with antibodies as indicated (BM: bone marrow, 15 µg protein per lane; PBMCs: peripheral blood mononuclear cells, 30 µg protein per lane; skin, 15 µg protein per lane; HFIs: hair follicles, 12 µg protein per lane). Top panel: densitometric analysis of relative p-eIF4E levels; Middle panel shows corresponding Western blots; Lower panel: equal amounts (12 µg protein) of tissues as indicated (PLT: platelets) were loaded to compare protein levels in different surrogate tissues. (B) Mean relative p-eIF4E levels in surrogate tissues from ICR mice collected at different time points post-dose (0.5 to 24 h) were assessed by Western blot; corresponding blots are shown on the right (V1: pooled vehicle samples (n=3) used to calculate 100%, V2: single sample from one vehicle-treated animal; “Set 1” refers to one sample set from those 3 replicates. (5 µg protein per lane for PBMCs, skin; 3 µg for HFIs).

anti-tumor activity when dosed in combination with a sub-optimal dose of dasatinib [1]. Tumors and normal tissues (HFIs, skin, PBMCs) were harvested after single doses of 12.5-200 mg/kg ETC-206. In tumor-bearing SCID mice, relative p-eIF4E levels at 2 h post-dose were significantly inhibited in all tissues (tumor, PBMCs, HFIs, skin) with a maximum inhibition of ~90% at the highest dose tested (200 mg). Tumor and skin were the most sensitive tissues, reaching ~70-75% inhibition at the lowest dose tested (12.5 mg/kg). Inhibition of p-eIF4E was significantly negative correlated with plasma concentrations for all tissues tested

($-0.55 \leq r \leq -0.80$, Figure 3C). However, p-eIF4E inhibition in tumor tissue was similar to that seen in skin at 12.5 mg/kg. PBMCs again showed highest variability in relative p-eIF4E levels. In summary, ETC-206 showed a linear dose-exposure relationship in both mouse strains tested, and a significant ($\geq 70\%$) inhibition of p-S209-eIF4E was seen in SCID mice with 12.5 mg/kg (corresponding to $\leq 3,500$ ng/mL or 8.6 µM). The observed inhibition in any tissue was never complete but on average around 80% from baseline levels. Maximal inhibition in all preclinical tissues was seen between 2-4 h post-dose.

Inhibition of p-eIF4E in human tissues

The same assay established using preclinical tissues was used to evaluate PD in clinical samples collected in the single ascending dose Ph1 FIH study in male, human HVs, as previously described [21]. ETC-206 was dosed in three different dosing periods (DPs) at 10 mg or 20 mg in the fasted state (DP1 or DP2, respectively), or at 10 mg in a fed state (DP3) to a total of 23 HVs as described [21]. PBMCs and HFs were collected at all DPs at up to 9 different time points (0-30 h). In DP3 additional pre-dose and a 1.5 h post-dose skin samples were analyzed from 9 donors. In contrast to mice,

no inhibition of p-eIF4E was observed in human PBMCs within the first 4 h after a single dose, however, inhibition was seen from 24 h onwards. At DP1, relative p-eIF4E levels showed an inhibition of 24%, which was statistically significant ($P=0.0037$; Figure 4A; S2A Figure). The heat map shows that at 24 h post-dose 11/16 subjects treated showed $\geq 15\%$ and up to 56% inhibition (Figure 4B). There was a linear trend for inhibition with a slope of -0.036 that was significant ($p=0.0043$). At DP2, an inhibition of $\geq 27\%$ up to 52% post-dose was seen with 8/14 subjects at 24 h, and $\geq 12\%$ up to 70% in 11/14 subjects at 30 h post-dose. There

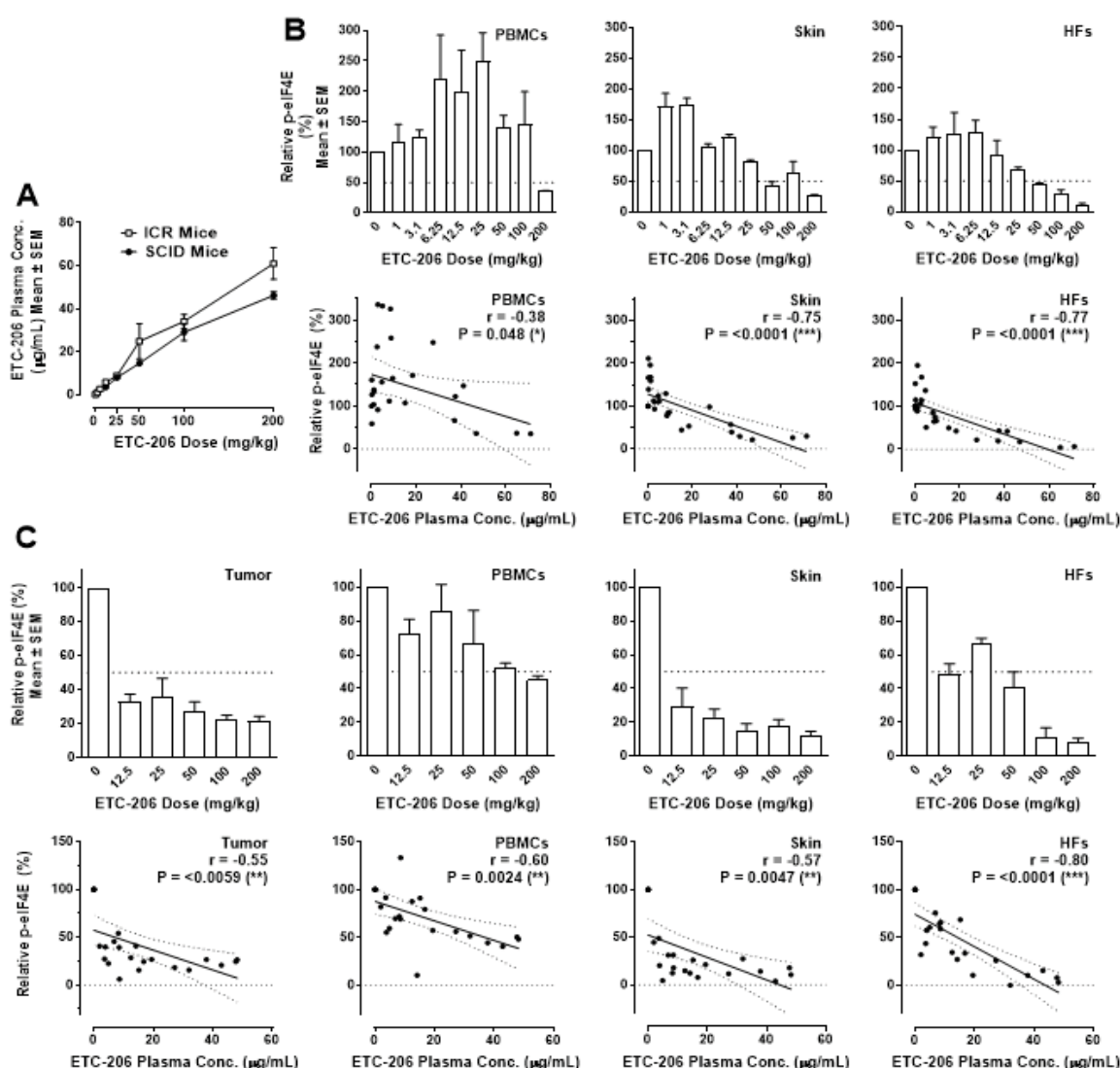


Figure 3: Plasma concentrations, relative p-eIF4E levels, and PK/PD correlations in tissues from ICR mice and tumor-bearing SCID mice after a single-dose of ETC-206. (A) Plasma concentrations of ETC-206 were determined by UPLC-MS/MS 2 h post-dose in female ICR ($n=3/\text{dose}$) and tumor-bearing female SCID mice ($n=4/\text{dose}$). Dose levels tested were 1, 3.1, 6.25, 12.5, 25, 50, 100, 200 mg/kg for ICR mice, 12.5, 25, 50, 100, 200 mg/kg for SCID mice. (B) Upper panels: mean relative p-eIF4E levels from surrogate tissues of ICR mice treated with ETC-206 for 2 h at the indicated dose levels were determined by Western blot followed by densitometry. Lower panels; correlation between ETC-206 plasma concentrations and p-eIF4E inhibition in individual animals ($n=27$); solid line: linear correlation, dotted lines: 95% confidence intervals, Pearson's r and corresponding P values are shown; (C) Upper panels and lower panels as described under (A) but in SCID mice bearing K562-eIF4E tumor ($n=4/\text{dose}$). Tumors collected had a mean volume of 422 mm^3 26 days post implantation.

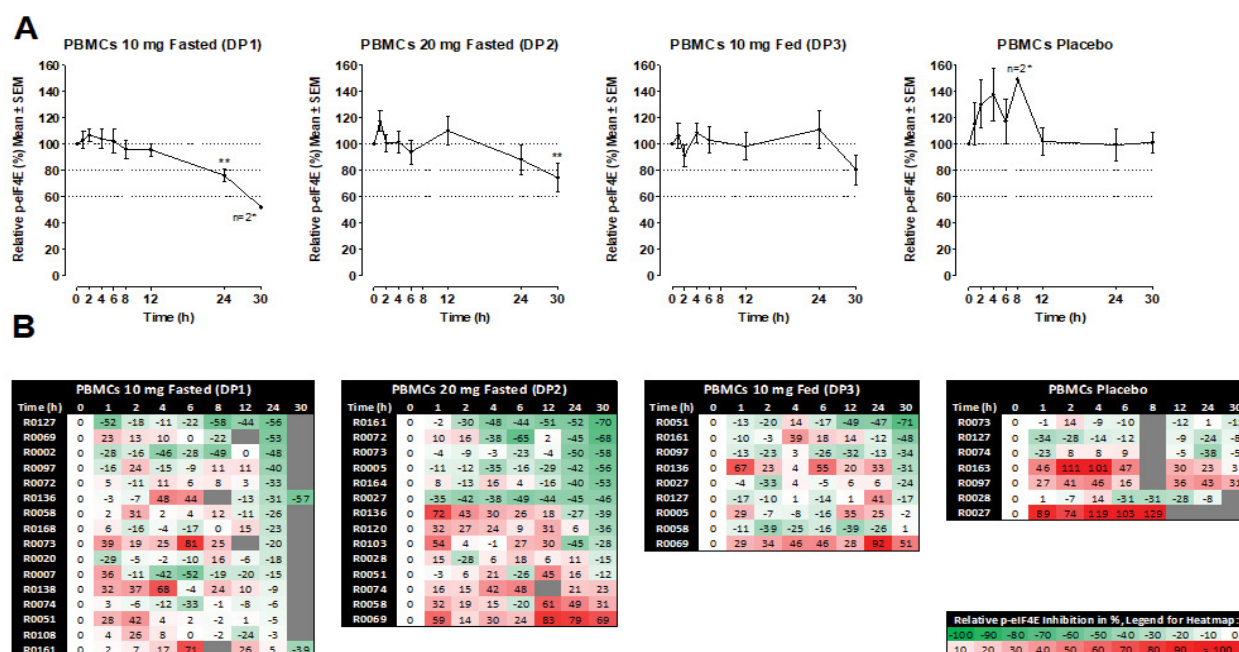


Figure 4: Effects of a single-dose of ETC-206 on relative p-eIF4E levels in PBMCs from human volunteers. Subjects (male HVs) were dosed with 10 mg (n=16) or 20 mg (n=14) ETC-206 in a fasted state, or with 10 mg (n=9) ETC-206 in fed state or received placebo (n=7). Whole blood was collected in CPT-vacutainers tubes with sodium citrate as anti-coagulant, at time points as indicated from pre-dose (0) to 24 h or 30 h (\pm 6 min). PBMCs were isolated and immediately snap-frozen. Relative p-eIF4E levels were determined in PBMCs as described for Figure 3B. (A) Mean relative p-eIF4E levels are shown per time point, for a time point with only n=2 no SEM is shown (as indicated by *). ** indicates $P < 0.005$, for the one-way ANOVA with Geisser-Greenhouse correction. (B) Heat map of relative p-eIF4E levels in PBMCs per dosing group and shaded according to the inhibition, see inserted legend; Grey fields without numbers indicate samples not collected, samples lost during analysis, or outliers.

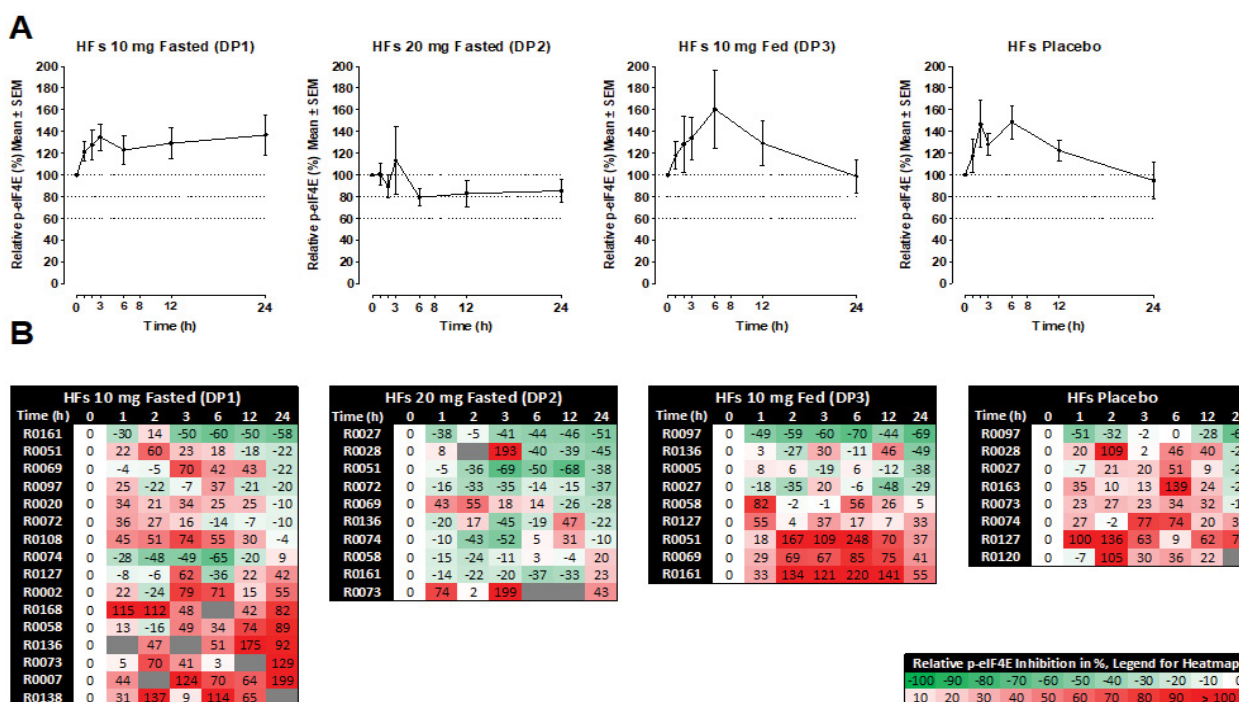


Figure 5: Effects of a single-dose of ETC-206 on the inhibition of relative p-eIF4E levels in hair follicles from human HVs. At least 40 HFs were collected at the indicated times (\pm 15 min). Western blot and densitometry were performed as described for Figure 3B, Samples from 4 volunteers had to be excluded from all analyses as the pre-dose sample did not yield any protein (not shown). For (A), (B), see legend for Figure 4.

was a statistically significant linear trend for inhibition with a slope of -0.051 ($p < 0.0001$). Similarly, for DP3, the maximum inhibition was seen at 30 h post-dose with inhibition $\geq 24\%$ up to 71% in samples from 5/9 subjects at 30 h but without linear trend for inhibition. In PBMCs of placebo treated subjects no mean inhibition was observed at any time point. In HFs at DP2, there was an approximately 20% inhibition observed from 6 h onwards, but no significant inhibition seen in HFs from subjects treated with 10 mg or placebo (Figure 5A and 5B; S2B Figure). Human skin, in contrast to murine skin, had much lower levels of total eIF4E and no change in the low amounts of p-eIF4E levels was observed. In addition, the observed protein size for p-eIF4E in human skin was variable (S2C Figure).

Comparing murine and human PK/PD relationships of ETC-206

Figure 6A shows the human plasma PK of ETC-206 over 72 h (for DP1) and over 144 h for the other two dosing groups (DP2, DP3), with sampling time points for biomarkers indicated by vertical lines. The T_{max} for the two groups dosed in fasted state (DP1, DP2) was about 1 h post-dose. The mean C_{max} for the 10 mg groups (DP1, DP3) was close to 1 $\mu\text{g/mL}$, and reached about 2 $\mu\text{g/mL}$ for the 20 mg group (DP2). A weak, non-significant negative correlation between C_{max} and p-eIF4E inhibition at 24 h post-dose was found when all individual data pairs were analyzed (DP1-DP3 and placebo, $n=46$), similarly the correlation between $AUC_{0-\infty}$ and p-eIF4E inhibition was slightly negative, but not statistically significant (Figure 6B). The PK profile of ETC-206 was compared between mouse and human using doses that are roughly comparable (5 mg/kg dose in mice is the human equivalent dose of 20 mg, Figure 6A, 6C). The C_{max} levels observed in human were below the 3,500 ng/mL threshold shown to cause acute p-eIF4E inhibition in SCID mice, but the plasma concentration remained above the *in vitro* IC_{50} for p-eIF4E inhibition in PBMCs of 1.7 μM (694 ng/mL) for 30 h (see Figure 6A). Due to a 14-fold higher mean half-life in human (Figure 6A, $t_{1/2} = 25.8$ h) compared to mice (Figure 6C, $t_{1/2} = 1.8$ h), the mean AUC_{0-t} was about 10x greater in human at comparable C_{max} (Figure 6D), which may explain the delayed p-eIF4E inhibition observed in the human study.

Discussion

Blocking cap-dependent mRNA translation selective and potent inhibitors of MNK has proven to provide clinical benefits for cancer patients with eFT508 being granted orphan drug status by FDA for further development in diffuse large B-cell lymphoma [19] and having shown favorable clinical results in the Ph2 trial in NSCLC in combination with pembrolizumab [20]. There is strong evidence that MNK inhibition blocks multiple oncogenic proliferation pathways, reduces pro-inflammatory and pro-tumorigenic cytokines,

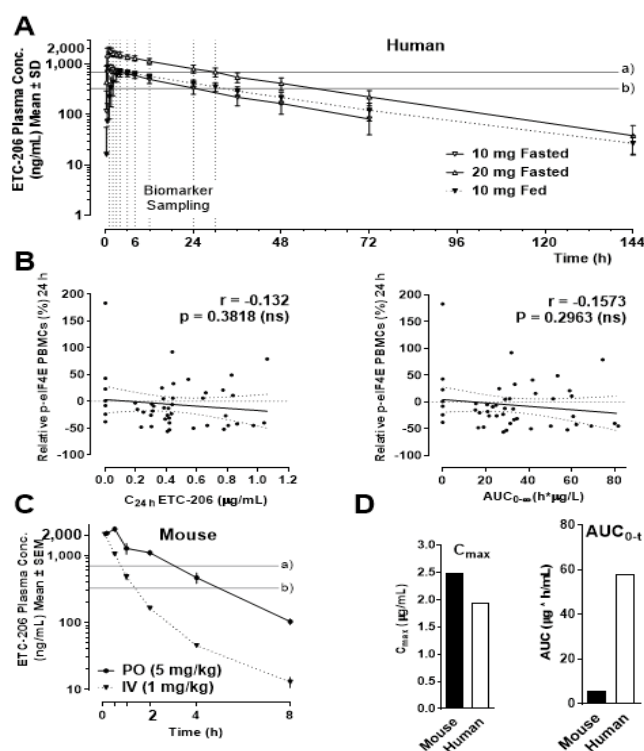


Figure 6: PK/PD comparison of ETC-206 in human HVs and ICR mice. (A) PK of ETC-206 in human plasma, indicating the time points of biomarker sampling (dotted vertical lines) For 10 mg fasted (DP1: $n=16$, except for the 30 h and the 144 h time point ($n=2$); for 20 mg fasted (DP2: $n=14$, except for 144 h ($n=11$); and for 10 mg fed group (DP3) $n=9$, except for 144 h ($n=7$)). The IC_{50} values for inhibition of eIF4E phosphorylation in human PBMCs (694 ng/mL), line a, and in K562-eIF4E cells (327 ng/mL), line b, are shown. (B) Correlation between relative levels p-eIF4E inhibition and plasma concentration at 24 h post-dose (left) or $AUC_{0-\infty}$ (right) in PBMCs at 24 h ($n=46$, lines, r and P : as described in Figure 3). (C) ETC-206 plasma concentrations were determined in ICR mice after oral (PO) or intravenous (IV) dosing of fasted at the time points indicated ($n=3$ /group). Lines a) and b) show the same p-eIF4E IC_{50} values as in Figure A. (D) Comparison of C_{max} and AUC_{0-t} in humans dosed with 20 mg ETC-206, fasted state) versus ICR mice, dosed at 5 mg/kg PO, ETC-206 (non-fasted).

while increasing anti-tumor immunity [22-24]. While cytotoxic activity has been described for non-specific MNK inhibitors *e.g.*, cercosporamide or CGP57380, selective MNK inhibitors *e.g.*, ETC-206, eFT508 and BAY 1143269 have very little anti-proliferative activity with cellular $IC_{50} > 30 \mu\text{M}$ in a majority of cell lines (S1 Table) [24, 25]. Besides ETC-206, only eFT508 and BAY 1143269 entered the clinic with BAY 1143269 being similar to ETC-206 in terms of potency for MNK and selectivity (MNK1 IC_{50} 40 nM, MNK2 IC_{50} 904 nM and PIM1 IC_{50} 518 nM), while eFT508 is a more potent MNK1/2 inhibitor (MNK1 IC_{50} 2.4 nM, MNK2 IC_{50} 1 nM and DRAK1 [STK17A] IC_{50} 82 nM) [25]. Comparing target efficacy (*i.e.*, p-eIF4E inhibition) in mice, ETC-206 is significantly more potent than BAY 1143269. The latter

led to only 46% inhibition of p-eIF4E in A549 tumors at approximately at T_{max} at 200 mg/kg at steady state [24], compared to 70% inhibition with 12.5 mg for ETC-206 after a single dose (Figure 3C). To draw a conclusion on the doses of ETC-206 required for PD inhibition in different murine tissues more weight was given to tumor and skin effects rather than PBMC effects, as the processing time was much faster and hence less variability was observed. The mouse PBMC extraction protocol is lengthy and involves several steps without added phosphatase inhibitor and has previously been demonstrated to show relatively higher variability compared to other murine tissues, while providing much better results in humans [26]. Target efficacy of eFT508 was tested in a B-cell lymphoma xenograft model, where a 1 mg/kg dose gave a 70% inhibition of p-eIF4E up to 8 h, but no inhibition was seen at 16 or 24 h post-dose (at a plasma C_{max} of ~200 nM), achieving comparable inhibition to ETC-206 at a dose of 12.5 mg/kg. In human patients BAY 1143269 at a dose of 10 mg gave a geometric mean plasma C_{max} of 12.7 $\mu\text{g/L}$ with an AUC_{0-24h} of 169 $\mu\text{g}\cdot\text{h/L}$ after a single dose, with dose escalation going up to 50 mg, yielding dose-proportional exposures [27]. ETC-206 at the same 10 mg dose (fasted) in human had a mean plasma C_{max} of 927 $\mu\text{g/L}$ and an AUC_{0-t} of 21,909 $\mu\text{g}\cdot\text{h/L}$ [21], demonstrating superior PK properties translated from mice to humans. The development of the BAY 1143269 has since been stopped.

For eFT508, the recommended human dose of 450 mg achieved an exposure of AUC_{0-24h} 7,800 $\mu\text{g}\cdot\text{h/L}$ and a C_{max} of 540 $\mu\text{g/L}$ after a single dose [19] with $t_{1/2}$ of 12 h. In the clinic, eFT508 was initially dosed as 450 mg of oral solution once daily, with dosing later changed to a twice daily 200 mg capsule formulation that has improved the AUC at steady state (increase from 5.4 to 10.9 $\text{h}\cdot\mu\text{g/mL}$). At steady state (on Day 15), eFT508 reported a mean 74% inhibition of p-eIF4E in PBMCs for up to 10 h but all other doses tested from 50 mg to 600 mg only lead to mean inhibition of 50-55% [19]. ETC-206 did not show p-eIF4E inhibition in human tissue within the first 6 h after a single dose and it was not expected, based on the C_{max} of 2,000 ng/mL as this did not reach the plasma concentration of 3,500 ng/mL that inhibited p-eIF4E in mouse tissues by ~70%. However, it is feasible that the long $t_{1/2}$ of ETC-206 and therefore the high AUC_{0-t} of ~ 60,000 $\mu\text{g}\cdot\text{h/L}$ (Figure 6D) contributed to the delayed onset of the p-eIF4E inhibition observed in PBMCs at a dose of 20 mg and to a lower extent at 10 mg. Based on work of Abronzo *et al.* and Eckerdt *et al.* it is also possible that there is a MNK-eIF4E feedback mechanism with contributions by PI3K and mTOR [28, 29] that could cause a delayed PD effect. However, we have no direct experimental evidence for that other than observing rapid initial p-eIF4E inhibition, followed by less inhibition at around 6 h and then more inhibition again between 8-12 h in mice (Figure 2), and

seeing delayed inhibition (at 24-30 h) in human samples after a single dose (Figure 4, Figure 5). ETC-206 now enters a clinical trial in cancer patients and it will be best to test for the expected early p-eIF4E inhibition in PBMCs at steady state to provide confirmatory clinical evidence of PD-inhibition. For the clinical development of ETC-206 it was essential to have the p-eIF4E assay sufficiently validated in preclinical species which allowed us to demonstrate that there is trend for delayed p-eIF4E inhibition in human PBMCs. Here, we have shown that ETC-206 is a selective MNK inhibitor that preclinically leads to dose-dependent PD inhibition in tumors as well as surrogate tissues. In human HVs ETC-206 showed excellent PK properties with a $t_{1/2}$ in humans amenable for every other day dosing and a trend of PD inhibition, which needs to be confirmed in the ongoing Ph2 trial.

Abbreviations

BSA: Bovine serum albumin; CML: Chronic myeloid leukemia; DP: dosing period; eIF4E: Eukaryotic initiation factor 4E; GLP: Good laboratory practice; HFs: Hair follicles; HV: Healthy volunteer; MAPK: Mitogen-activated protein kinase; ICR: Institute of Cancer research; IRB: Institutional Review Board; MNK: MAPK interacting kinase; Na-CMC: Sodium carboxymethyl cellulose; NAELAR: National Advisory Committee for Laboratory Animal Research; NIH: National Institutes of Health; NSCLC: Non-small cell lung cancer; p-eIF4E: Phosphorylated eIF4E; PBMC: Peripheral blood mononuclear cells; PD: Pharmacodynamic; PD-1: Programmed cell death protein 1; PD-L1: Programmed death ligand 1; Ph1/2: Phase 1/2; PK: Pharmacokinetic; S209: Serine 209; SCID: Severe combined immunodeficiency.

Acknowledgements

This study was supported by the Biomedical Research Council (BMRC) A*STAR (SPF2012/002), the BMS Open Collaborative Fund (OCF) approved by the National Research Foundation in Singapore (13/1/85/18/693), and the National Medical Research Council (NMRC) of Singapore (MH95:03/7-6) all awarded to the D3 Platform (now EDDC) and scientifically supported by Alex Matter. Shu Jing Lim is acknowledged for her technical support.

Conflict of interest

The authors of the manuscript declare no conflict of interest.

Supplementary Data: https://www.fortunejournals.com/supply/JCSCT_11218.pdf

References

1. Yang H, Chennamaneni LR, Ho MWT, et al. Optimization of Selective Mitogen-Activated Protein Kinase Interacting Kinases 1 and 2 Inhibitors for the Treatment of Blast Crisis Leukemia. *J Med Chem* 61 (2018): 4348-4369.

2. Dreaz A, Mikulski M, Milik M, et al. Mitogen-activated Protein Kinase (MAPK) Interacting Kinases 1 and 2 (MNK1 and MNK2) as Targets for Cancer Therapy: Recent Progress in the Development of MNK Inhibitors. *Curr Med Chem* 24 (2017): 3025-3053.
3. Joshi S, Plataniias LC. Mnk kinase pathway: Cellular functions and biological outcomes. *World J Biol Chem* 5 (2014): 321-333.
4. Shveygert M, Kaiser C, Bradrick SS, et al. Regulation of eukaryotic initiation factor 4E (eIF4E) phosphorylation by mitogen-activated protein kinase occurs through modulation of Mnk1-eIF4G interaction. *Mol Cell Biol* 30 (2010): 5160-5167.
5. Hay N. Mnk earmarks eIF4E for cancer therapy. *Proc Natl Acad Sci U S A* 107 (2010): 13975-13976.
6. Hou J, Lam F, Proud C, et al. Targeting Mnk for cancer therapy. *Oncotarget* 3 (2012): 118-131.
7. Ueda T, Watanabe-Fukunaga R, Fukuyama H, et al. Mnk2 and Mnk1 are essential for constitutive and inducible phosphorylation of eukaryotic initiation factor 4E but not for cell growth or development. *Mol Cell Biol* 24 (2004): 6539-6549.
8. Graff JR, Konicek BW, Vincent TM, et al. Therapeutic suppression of translation initiation factor eIF4E expression reduces tumor growth without toxicity. *J Clin Invest* 117 (2007): 2638-2648.
9. Wendel HG, Silva RL, Malina A, et al. Dissecting eIF4E action in tumorigenesis. *Genes Dev* 21 (2007): 3232-3237.
10. Furic L, Rong L, Larsson O, et al. eIF4E phosphorylation promotes tumorigenesis and is associated with prostate cancer progression. *Proc Natl Acad Sci U S A* 107 (2010): 14134-14139.
11. Topisirovic I, Ruiz-Gutierrez M, Borden KL. Phosphorylation of the eukaryotic translation initiation factor eIF4E contributes to its transformation and mRNA transport activities. *Cancer Res* 64 (2004): 8639-8642.
12. Bhat M, Robichaud N, Hulea L, et al. Targeting the translation machinery in cancer. *Nat Rev Drug Discov* 14 (2015): 261-278.
13. Robichaud N, del Rincon SV, Huor B, et al. Phosphorylation of eIF4E promotes EMT and metastasis via translational control of SNAIL and MMP-3. *Oncogene* 34 (2015): 2032-2042.
14. Joshi S, Plataniias LC. Mnk Kinases in Cytokine Signaling and Regulation of Cytokine Responses. *Biomol Concepts* 3 (2012): 127-139.
15. Xu Y, Poggio M, Jin HY, et al. Translation control of the immune checkpoint in cancer and its therapeutic targeting. *Nat Med* 25 (2019): 301-311.
16. Robichaud N, Hsu BE, Istomine R, et al. Translational control in the tumor microenvironment promotes lung metastasis: Phosphorylation of eIF4E in neutrophils. *Proc Natl Acad Sci U S A* 115 (2018): 2202-2209.
17. Salvador-Bernaldez M, Mateus SB, Del Barco Barrantes I, et al. p38alpha regulates cytokine-induced IFNgamma secretion via the Mnk1/eIF4E pathway in Th1 cells. *Immunol Cell Biol* 95 (2017): 814-823.
18. Andersson K, Sundler R. Posttranscriptional regulation of TNFalpha expression via eukaryotic initiation factor 4E (eIF4E) phosphorylation in mouse macrophages. *Cytokine* 33 (2006): 52-57.
19. Falchook GS, Infante JR, Meric-Bernstam F, et al. A phase 1 dose escalation study of eFT508, an inhibitor of mitogen-activated protein kinase-interacting serine/threonine kinase-1 (MNK-1) and MNK-2 in patients with advanced solid tumors. *Journal of Clinical Oncology* 35 (2017).
20. El-Khoueiry AB, Tchekmedyian N, Sanborn RE, et al. A phase II, open-label study of tomivosertib (eFT508) added on to continued checkpoint inhibitor therapy in patients (pts) with insufficient response to single-agent treatment. *Journal of Clinical Oncology* 38 (2020).
21. Teneggi V, Novotny-Diermayr V, Lee LH, et al. First-in-Human, Healthy Volunteers Integrated Protocol of ETC-206, an Oral Mnk 1/2 Kinase Inhibitor Oncology Drug. *Clin Transl Sci* (2019).
22. Goel VK, Sharma RK, Staunton J, et al. Abstract LB-068: Tomivosertib (eFT508), a potent and highly selective inhibitor of MNK1 and MNK2, enhances CAR T cell activity through modulating T cell differentiation. *Cancer Research* 79 (2019): LB-068.
23. Sharma RK, Goel VK, Staunton J, et al. A potent and highly selective inhibitor of MNK1 and MNK2, regulates T-cell differentiation promoting an antitumor immune response. *Cancer Research* 78 (2018): 5546.
24. Santag S, Siegel F, Wengner AM, et al. BAY 1143269, a novel MNK1 inhibitor, targets oncogenic protein expression and shows potent anti-tumor activity. *Cancer Lett* 390 (2017): 21-29.
25. Reich SH, Sprengeler PA, Chiang GG, et al. Structure-based Design of Pyridone-aminal eFT508 Targeting Dysregulated Translation by Selective Mitogen-activated Protein Kinase Interacting Kinases 1 and 2 (MNK1/2) Inhibition. *J Med Chem* (2018).

Citation: Bong Hwa Gan, Lay Hoon Lee, Reika Takeda, Maryam Yasin, Vincenzo Teneggi, Kantharaj Ethirajulu, Pauline Yeo, Dhananjay Umrani, Vishal Pendharkar, Darren Wan Teck Lim, Greg Li, Qingshu Lu, Yang Cao, Ranjani Nellore, Stephanie Blanchard, Hannes Hentze, Veronica Novotny-Diermayr. Pharmacodynamic Evaluation of AUM001/Tinodasertib, an Oral Inhibitor of Mitogen-Activated Protein Kinase (MAPK)-Interacting Protein Kinase 1, 2 (MNK1/2) in Preclinical Models and Tissues from a Phase 1 Clinical Study. *Journal of Cancer Science and Clinical Therapeutics*. 8 (2024): 254-264.

26. Novotny-Diermayr V, Sausgruber N, Loh YK, et al. Pharmacodynamic evaluation of the target efficacy of SB939, an oral HDAC inhibitor with selectivity for tumor tissue. *Mol Cancer Ther* 10 (2011): 1207-1217.
27. Clinical Trial Results Synopsis: An open-label, non-randomized, multicenter Phase I study to characterize the safety, tolerability, pharmacokinetics, pharmacodynamics, and maximum tolerated dose of oral MKNK1 inhibitor BAY 1143269 given alone or in combination with intravenous docetaxel in subjects with advanced solid tumors. Bayer (2018).
28. D'Abronzio LS, Ghosh PM. eIF4E Phosphorylation in Prostate Cancer. *Neoplasia* 20 (2018): 563-573.
29. Eckerdt F, Beauchamp E, Bell J, et al. Regulatory effects of a Mnk2-eIF4E feedback loop during mTORC1 targeting of human medulloblastoma cells. *Oncotarget* 5 (2014): 8442-8451.